

Coexistence of fast and slow luminescence in three-dimensional Si/Si<sub>1-x</sub>Ge<sub>x</sub> nanostructures

B. V. Kamenev and L. Tsybeskov\*

*Department of Electrical and Computer Engineering, New Jersey Institute of Technology, University Heights, Newark, New Jersey 07102*

J.-M. Baribeau and D. J. Lockwood

*Institute for Microstructural Sciences, National Research Council, Ottawa, KIA 0R6, Canada*

(Received 15 September 2005; published 18 November 2005)

We report an experimental observation of both a fast ( $\sim 10 \mu\text{s}$ ) and a slow ( $\sim 10 \text{ms}$ ) photoluminescence (PL) that coexist in Ge-rich ( $x > 0.5$ ) islandlike, three-dimensional Si/Si<sub>1-x</sub>Ge<sub>x</sub> nanostructures. We present a quantitative model that explains the observed PL lifetime dependence on carrier concentration, temperature, and detection wavelength. The PL dynamics are found to be determined by the excess carrier concentration: the fast PL is associated with a dynamic type I and the slow PL with a type II energy band alignment in Ge-rich Si/SiGe nanostructures.

DOI: [10.1103/PhysRevB.72.193306](https://doi.org/10.1103/PhysRevB.72.193306)

PACS number(s): 78.67.Hc, 78.67.Pt

Over the last decade, continued progress in the development of high-quality three-dimensional (3D) Si/Si<sub>1-x</sub>Ge<sub>x</sub> heterostructures (i.e., self-organized clusters and islands) has been focused on the realization of Si-based optoelectronic devices, e.g. infrared detectors and light-emitting diodes (LED) operating at 1.3-1.6  $\mu\text{m}$ .<sup>1-5</sup> The most serious limitation for SiGe LED applications is the low photo- and electroluminescence (PL and EL) quantum efficiency at room temperature.<sup>6,7</sup> It has been shown that in Si-rich SiGe alloys, excitons are localized at random alloy fluctuations, and the PL quantum efficiency at low temperatures with a low excitation intensity can be  $\sim 10\%$ .<sup>8</sup> The exciton localization at random SiGe alloy fluctuations is of little practical importance, mainly because of its low binding energy  $\sim 20 \text{meV}$ , and the PL is thermally quenched at temperatures  $> 40 \text{K}$ .<sup>8-10</sup> In contrast, the fabrication of high-quality Ge-rich SiGe islands embedded into a Si matrix is expected to increase the PL quantum efficiency at elevated temperatures: the energy band discontinuities should localize electron-hole pairs within dislocation-free, nanometer-size Si<sub>1-x</sub>Ge<sub>x</sub> islands with  $x > 0.5$ . An important advantage of 3D Si/Si<sub>1-x</sub>Ge<sub>x</sub> nanostructures is the ability to decrease strain due to their surface morphology, and increase the critical thickness and the Ge content  $x$ .<sup>3</sup> However, the electron-hole spatial confinement critically depends on the energy band alignment, and most of the Si/SiGe structures are believed to exhibit a type II heterointerface where electrons and holes are spatially separated with a limited wave function overlap.<sup>11,12</sup> At the same time, several studies have independently claimed the existence of quasitype I energy band alignments in Si/SiGe nanostructures.<sup>12-14</sup> This controversy can be resolved using PL lifetime measurements since a fast PL decay is expected for spatially confined (type I heterointerface) and a slow PL decay for spatially separated (type II heterointerface) electrons and holes. In this work, we present a comprehensive investigation of the PL dynamics covering up to five decades of both intensity and time in molecular beam epitaxy (MBE) grown Si/Si<sub>1-x</sub>Ge<sub>x</sub> 3D (i.e., islandlike) nanostructures with  $x$  controllably varying from 0.16 to 0.55. We show that the PL lifetime is strongly dependent on the excitation conditions,

and that it can be stretched over three decades, from 10  $\mu\text{s}$  to 10 ms. We conclude that the actual energy band alignment in Ge-rich ( $x > 0.5$ ) structures is interestingly determined by the excess carrier concentration and that the recombination of both spatially confined and spatially separated carriers takes place.

The samples used in this study were grown by MBE in a VG Semicon V80 system using a methodology described elsewhere.<sup>15,16</sup> The structures investigated consist of 15 periods of Si<sub>0.84</sub>Ge<sub>0.16</sub>(7.0 nm)/Si(34.0 nm) grown at 600 °C, 10 periods of Si<sub>0.47</sub>Ge<sub>0.53</sub>(3.5 nm)/Si(14.9 nm) grown at 625 °C, and 10 periods of Si<sub>0.45</sub>Ge<sub>0.55</sub>(3.0 nm)/Si(13.1 nm) grown at 640 °C. The Si<sub>1-x</sub>Ge<sub>x</sub> nominal composition  $x$  and layer thicknesses in the multilayers were estimated from x-ray rocking curves analysis and were found consistent with the shutter time sequencing and atomic fluxes (typically in the range 0.05–0.1  $\text{nms}^{-1}$ ) used during deposition. Transmission electron microscopy (TEM) studies have shown, however, that the Si/Si<sub>1-x</sub>Ge<sub>x</sub> multilayers exhibit an islandlike morphology (i.e., 3D growth) with vertically aligned Si<sub>1-x</sub>Ge<sub>x</sub> undulations.<sup>17,18</sup> The quality of the Si/Si<sub>1-x</sub>Ge<sub>x</sub> interfaces was also investigated: X-ray reflection and Raman measurements indicated that samples had chemically abrupt interfaces, despite the 3D morphology.<sup>18</sup>

The PL signal was excited by a pulsed laser diode with wavelength of 680 nm, dispersed using a single grating Acton Research 0.5 m monochromator and recorded using a Hamamatsu photomultiplier in the spectral range of 0.9–1.63  $\mu\text{m}$  (0.76–1.38 eV) and a LeCroy 915M digital oscilloscope using averaging over 1000 pulses. The background signal has been independently measured and carefully subtracted. The excitation pulse duration was chosen to achieve steady-state PL conditions. The overall time resolution of the entire system was better than 500 ns. The cw PL was excited using an Ar<sup>+</sup> laser (458 nm) and detected by a liquid nitrogen cooled InGaAs diode array (0.9-1.6  $\mu\text{m}$ /0.77–1.38 eV), or a single, liquid nitrogen cooled, InGaAs detector with a spectral sensitivity extending up to 2.6  $\mu\text{m}$  (0.48 eV). The PL measurements were performed in the temperature range of 4-300 K.

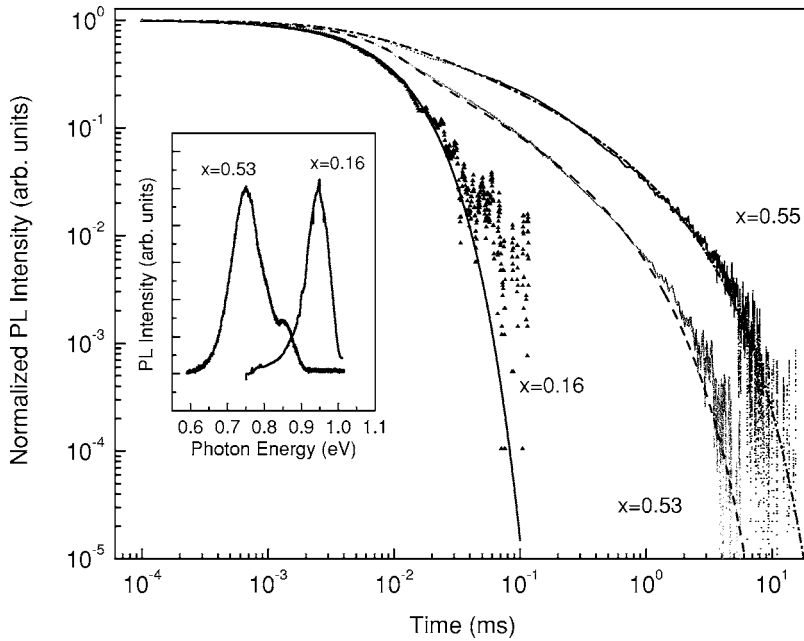


FIG. 1. Low-temperature (4 K) PL transients in 3D  $\text{Si}/\text{Si}_{1-x}\text{Ge}_x$  nanostructures with different Ge concentrations (note the double logarithmic scale). The inset shows PL spectra at 4 K for samples with  $x=0.16$  and  $x=0.53$ . For the Si-rich  $\text{Si}/\text{Si}_{1-x}\text{Ge}_x$  sample with  $x=0.16$ , the PL decay is well described by a single exponential fit (solid line) with  $\tau \approx 9 \mu\text{s}$ . For Ge-rich  $\text{Si}/\text{Si}_{1-x}\text{Ge}_x$  samples with  $x=0.53$  and  $x=0.55$ , the PL decay fit (dash and dash-dot lines) is obtained using Eq. (3) with an energy barrier of  $\sim 1.7$  and  $2.0$  meV, respectively.

Figure 1 compares low-temperature cw PL spectra (see the inset) and PL transients for  $\text{Si}/\text{Si}_{1-x}\text{Ge}_x$  samples with a different Ge composition in the time domain from 100 ns to 50 ms. A sample with  $x=0.16$  exhibits a PL spectrum peaked at  $\sim 0.97$  eV and a monoexponential PL decay with the lifetime of  $\sim 9 \mu\text{s}$  (see the fit shown in Fig. 1). The PL spectra of  $\text{Si}_{1-x}\text{Ge}_x/\text{Ge}$  samples with  $x=0.53$  and  $x=0.55$  are similar, with a major PL peak at  $\sim 0.75$  eV. Their PL decays are qualitatively similar: both transients show fast (microsecond) and slow (millisecond) PL components. The data cannot be fitted by a simple superposition of two exponents due to the existence of an intermediate region (from 100 to 500  $\mu\text{s}$ ), where the carrier lifetime is a function of the carrier concentration, as discussed below.

The photon energy dependencies of the PL relaxation times are summarized in Fig. 2. The fast PL is nearly the same in all  $\text{Si}_{1-x}\text{Ge}_x/\text{Ge}$  samples with  $0.16 < x < 0.55$ : the lifetime ranges from 3 to 20  $\mu\text{s}$  and shows no significant dependence on the detection wavelength in the spectral range of 0.75–0.82 eV. In contrast, the slow PL component is found only in samples with  $x > 0.5$ , and it exhibits a strong, nearly exponential dependence on the detection wavelength. The characteristic PL lifetime at the longest detected wavelengths slows down to 1 ms in the sample with  $x=0.53$  and down to 10 ms in the sample with  $x=0.55$  (see Fig. 2).

The PL temperature dependence in  $\text{Si}/\text{Si}_{1-x}\text{Ge}_x$  samples with  $x=0.16$  exhibits a 15–20 meV activation energy for both the PL lifetime shortening and the PL intensity thermal quenching (not shown). In samples with  $x > 0.5$ , the fast PL component has an activation energy of  $\sim 20$  meV, which is similar to that of the  $x=0.16$  sample. The slow PL intensity exhibits thermal quenching with an activation energy of  $\sim 60$  meV, while its lifetime integrated over the spectral range of 0.75–0.85 eV decreases at elevated temperatures with an activation energy of 34 meV (Fig. 3). The significance of this observation will be discussed later. Also, we find that the PL decay in samples with  $x=0.16$  is independent of the excitation intensity (not shown), but in samples with

$x > 0.5$  the dependence is significant (Fig. 4).

First, we discuss the fast (microsecond lifetime) PL. Both Si and Ge are indirect band gap semiconductors with a millisecond lifetime for band-to-band carrier recombination at a low temperature.<sup>19</sup> Defect recombination (e.g., via dangling bonds, etc.) is reported to have a nanosecond lifetime.<sup>20</sup> A nanosecond PL has also been found in pseudomorphic SiGe quantum well structures and is believed to be controlled by nonradiative recombination processes.<sup>21</sup> Complex excitons in  $\text{Si}/\text{SiGe}$  heterostructures associated with the four in-plane electron valleys and the two valleys along the growth direction<sup>22</sup> might lead to the coexistence of fast and slow PL: however, the applicability of the model developed for a two-dimensional (i.e., planar)  $\text{Si}/\text{Si}_{1-x}\text{Ge}_x$  heterosystem to a three-dimensional (i.e., islandlike) morphology has not been established. Therefore, we conclude that the fast PL with a

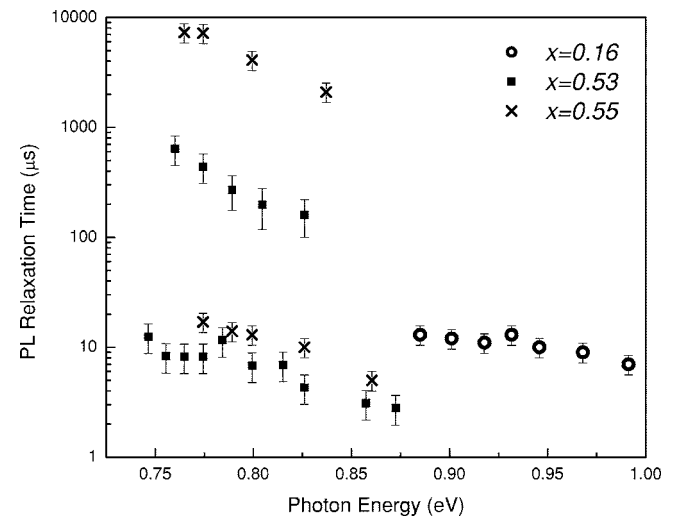


FIG. 2. The PL relaxation time constant as a function of the PL detection photon energy for  $\text{Si}/\text{Si}_{1-x}\text{Ge}_x$  samples with  $0.16 \leq x \leq 0.55$ . All measurements were performed at 4 K under  $\sim 3 \text{ W}/\text{cm}^2$  excitation.

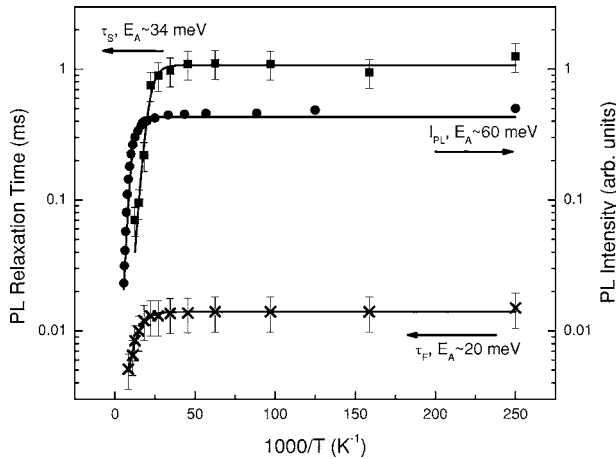


FIG. 3. Slow and fast PL time constants and PL intensity as functions of inverse temperature for Si/Si<sub>1-x</sub>Ge<sub>x</sub> samples with  $x = 0.53$ . The calculated activation energies are shown. The excitation intensity was  $\sim 3 \text{ W/cm}^2$ .

lifetime of 3–20  $\mu\text{s}$  observed in 3D Si/Si<sub>1-x</sub>Ge<sub>x</sub> samples with  $0.16 \leq x \leq 0.55$  is associated with the recombination of excitons localized on compositional fluctuations within SiGe islands. The experimentally observed thermal quenching with an activation energy of 15–20 meV in the PL intensity temperature dependence thus a measure of the exciton binding energy.<sup>23,24</sup>

Slow PL is found in Ge-rich Si/Si<sub>1-x</sub>Ge<sub>x</sub> samples with  $x > 0.5$ , and it has a very long lifetime (up to 10 ms). This lifetime is considerably longer than that for band gap PL in bulk Si and Ge,<sup>19</sup> and it can be explained by a recombination of spatially separated carriers (i.e., type II energy band alignment) at the Si/Si<sub>1-x</sub>Ge<sub>x</sub> heterointerface with a potential well for holes and a potential barrier for electrons in the Si<sub>1-x</sub>Ge<sub>x</sub> region. Furthermore, it has been proposed that in MBE-grown Si<sub>1-x</sub>Ge<sub>x</sub> samples with  $x > 0.5$ , Ge segregation may occur.<sup>25</sup> In samples with  $x$  increasing from 0.53 to 0.55, this process leads to (i) an increase in the height of the potential barriers for electrons at the Si/Si<sub>1-x</sub>Ge<sub>x</sub> interface; (ii) a decrease of the overlap of electron-hole wave functions; and

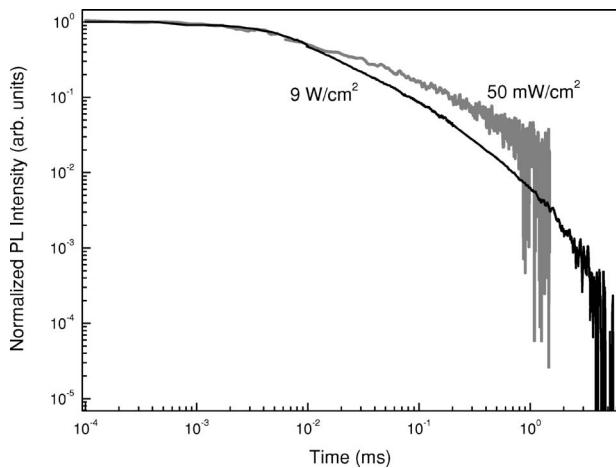


FIG. 4. Normalized PL transients in a Si/Si<sub>1-x</sub>Ge<sub>x</sub> sample with  $x = 0.53$  under low (gray) and high (black) intensity excitations.

(iii) an increase of the PL radiative lifetime. In this model, the probability of electron-hole recombination should exhibit an exponential dependence on the barrier parameters, as well as on the Ge composition in Si<sub>1-x</sub>Ge<sub>x</sub> islands. In addition, the strong dependence found in the slow PL lifetime as a function of the detection wavelength can be explained as follows: a larger band offset for electrons corresponds to a lower PL photon energy and a longer PL lifetime (see Fig. 2). Our results suggest that significant modifications of the Si/Si<sub>1-x</sub>Ge<sub>x</sub> heterointerface energy band alignment occur when  $x > 0.5$ . However, as  $x$  is approaching 0.6, strain and strain-induced diffusion strongly increase.<sup>26</sup> Further analysis of the energy band alignment, microstructure, and properties of Si<sub>1-x</sub>Ge<sub>x</sub> cluster samples with  $0.55 > x > 0.6$  will be presented elsewhere.<sup>26</sup>

In a coupled system with a type II energy band alignment and electrons localized at Si/Si<sub>1-x</sub>Ge<sub>x</sub> interfaces and/or within the Si<sub>1-x</sub>Ge<sub>x</sub> islands, the electron population is determined by Boltzmann statistics, where the energy barrier is equal to the conduction band offset. The complexity of the PL dynamics is determined by the competition between recombination channels involving electrons localized at the Si/Si<sub>1-x</sub>Ge<sub>x</sub> interfaces (lower-energy states, slower recombination) and within Si<sub>1-x</sub>Ge<sub>x</sub> islands (upper energy states, faster recombination). The temperature dependence of the PL radiative lifetime is explained as follows: at higher temperatures, the population of the upper energy states increases and the overall PL lifetime decreases. Under a relatively high level of photoexcitation, the spatially separated electrons and holes induce a band bending, which effectively lowers the electron energy barrier. Thus, the electron population of the upper states is a function of both the carrier concentration and the temperature. The process of carrier recombination can be modeled as

$$\frac{\partial N}{\partial t} = -\frac{N_S}{\tau_S} - \frac{N_F}{\tau_F}, \quad (1)$$

with  $N_{t=0} = N_0$ , where the number of carriers  $N = N_S + N_F$  and indices “S” and “F” refer to the slow and fast lifetimes ( $\tau_S$  and  $\tau_F$ , respectively) of carriers correspondingly localized at the lower (Si/Si<sub>1-x</sub>Ge<sub>x</sub> interface) and upper (Si<sub>1-x</sub>Ge<sub>x</sub> island) energy states.

The electron populations of fast ( $N_F$ ) and slow ( $N_S$ ) energy levels are related by Boltzmann statistics:

$$N_F = N_S e^{-E_B(N)/kT}, \quad (2)$$

where  $E_B(N)$  is the electron barrier height. Thus, we can rewrite Eq. (1) as

$$\frac{\partial N}{\partial t} = -\frac{N}{1 + e^{-E_B(N)/kT}} (\tau_S^{-1} + \tau_F^{-1} e^{-E_B(N)/kT}). \quad (3)$$

In addition to radiative carrier recombination, nonradiative recombination (e.g., via dangling bonds, etc.) has to be taken into account. Usually, the competition between temperature-independent radiative transitions and temperature-dependent nonradiative transitions for both recombination rates  $\tau_S^{-1}$  and  $\tau_F^{-1}$  is described by

$$\tau_{S,F}^{-1} = \tau_{R,(S,F)}^{-1} + \tau_{NR,(S,F)}^{-1} e^{-E_A/kT}, \quad (4)$$

where indices “R” and “NR” refer to radiative and nonradiative recombination rate constants and  $E_A$  is the activation energy for nonradiative recombination.

At a fixed temperature, the transparency of the electron barrier is simply a function of the carrier concentration. The fast channel of carrier recombination dominates at a high carrier concentration, and electron-hole recombination mainly involves electrons from upper energy states (i.e., within  $\text{Si}_{1-x}\text{Ge}_x$  islands) with a characteristic lifetime  $\tau_F$ . As the carrier concentration decreases, the transparency of the electron barrier decreases. Therefore, in our experiments we observe the intermediate regime in the PL decay (50–500  $\mu\text{s}$ ), where the PL lifetime is in the process of changing from  $\tau_F$  to  $\tau_S$ . This dynamic picture can be modeled, assuming an ideal Si/SiGe heterointerface with a triangular electron barrier, whose effective height is determined as  $E_B(N) = E_0 - C\sqrt{N}$ , where  $E_0$  is the conduction band offset and  $C$  is an adjustable parameter. Using values of  $\tau_F$  and  $\tau_S$  determined from the experimental data and  $E_0$  and  $C$  as fitting parameters, we obtained fits that are in excellent agreement with the experimental data for almost five decades in PL intensity over a very wide 100 ns–50 ms time domain (see Fig. 1).

This model can also be used to estimate the conduction band offset under quasi-steady-state conditions. In the case of low-intensity photoexcitation, the energy barrier dependence on carrier concentration can be ignored. In our experiments, this is a regime where the carrier concentration drops by at least two orders in magnitude, resulting in an insignificant energy band bending (i.e., very low excitation intensity

and a slow PL regime). Using Eqs. (3) and (4), we fitted the experimental data and obtained a conduction band energy offset of  $\leq 10$  meV, which is an upper estimate due to the assumption of an extremely low excess carrier concentration.

According to our analysis, the fast PL component dominates in Si/Si $_{1-x}$ Ge $_x$  heterostructures with type II energy band alignment when a significant energy band bending is induced by the excess carriers produced under high photoexcitation. Indeed, by decreasing the excitation intensity we can markedly suppress the fast PL component, (see Fig. 4). However, in practical measurements (i.e., at a higher excess carrier concentration), most of the carriers recombine via a fast recombination channel associated with dynamic (i.e., induced by carrier accumulation) type I energy band alignment, while the type II energy band alignment can only be confirmed by observing a slow PL decay at a low level of photoexcitation.

In conclusion, using time-resolved PL measurements in a time domain from 100 ns to 50 ms, we observe fast and slow PL components in Si/Si $_{1-x}$ Ge $_x$  3D nanostructures with  $x > 0.5$ . By assuming that carriers accumulate at Si/SiGe heterointerfaces (e.g., Si $_{1-x}$ Ge $_x$  island borders), we can fit PL transients over five decades, explain their temperature and spectral dependencies, and estimate the discontinuity in the conduction energy band at the Si/Si $_{1-x}$ Ge $_x$  heterointerface. In our model, the dynamic type I energy band alignment is induced by a high carrier concentration, while at a low carrier concentration recombination is controlled by the overlap of wave functions of spatially separated electrons and holes (i.e., type II energy band alignment).

The work at NJIT is supported by Intel Corp., the National Science Foundation, and the Foundation at NJIT.

\*Electronic mail: tsybesko@adm.njit.edu

<sup>1</sup>J. Tersoff *et al.*, Phys. Rev. Lett. **76**, 1675-1678 (1996).

<sup>2</sup>V. Holy *et al.*, Phys. Rev. Lett. **83**, 356 (1999).

<sup>3</sup>F. M. Ross, J. Tersoff, and R. M. Tromp, Phys. Rev. Lett. **80**, 984-987 (1998).

<sup>4</sup>Y. Shiraki *et al.*, Appl. Surf. Sci. **102**, 263 (1996).

<sup>5</sup>J. C. Sturm *et al.*, Phys. Rev. Lett. **66**, 1362 (1991).

<sup>6</sup>R. Apetz *et al.*, Appl. Phys. Lett. **66**, 445 (1995).

<sup>7</sup>Q. Mi *et al.*, Appl. Phys. Lett. **60**, 3177 (1992).

<sup>8</sup>L. C. Lenchyshyn *et al.*, Appl. Phys. Lett. **60**, 3174 (1992).

<sup>9</sup>H. Sunamura *et al.*, Appl. Phys. Lett. **66**, 953 (1995).

<sup>10</sup>A. I. Yakimov *et al.*, Phys. Rev. B **63**, 045312 (2001).

<sup>11</sup>R. People, IEEE J. Quantum Electron. **QE22**, 1696 (1986).

<sup>12</sup>M. L. W. Thewalt *et al.*, Phys. Rev. Lett. **79**, 269 (1997).

<sup>13</sup>T. Baier *et al.*, Phys. Rev. B **50**, 15191 (1994).

<sup>14</sup>D. C. Houghton *et al.*, Phys. Rev. Lett. **75**, 866-869 (1995).

<sup>15</sup>J.-M. Baribeau *et al.*, J. Appl. Phys. **63**, 5738 (1988).

<sup>16</sup>J.-M. Baribeau *et al.*, Thin Solid Films **183**, 17 (1989).

<sup>17</sup>N. L. Rowell *et al.*, J. Appl. Phys. **74**, 2790 (1993).

<sup>18</sup>H. K. Shin *et al.*, Solid State Commun. **114**, 505 (2000).

<sup>19</sup>M. L. W. Thewalt, in *Excitons*, edited by E. I. Rashba, and M. D. Sturge (North-Holland, Amsterdam, 1982), p. 393.

<sup>20</sup>S. Fukatsu *et al.*, Appl. Phys. Lett. **68**, 1889 (1996).

<sup>21</sup>A. Zrenner *et al.*, Phys. Rev. B **52**, 16608 (1995).

<sup>22</sup>C. Penn *et al.*, Phys. Rev. B **59**, 13314 (1999).

<sup>23</sup>N. L. Rowell *et al.*, J. Appl. Phys. **74**, 2790 (1993).

<sup>24</sup>K. Kawaguchi *et al.*, Appl. Phys. Lett. **81**, 817 (2002).

<sup>25</sup>B. V. Kamenev *et al.*, Appl. Phys. Lett. **84**, 1293 (2004).

<sup>26</sup>B. V. Kamenev *et al.* (unpublished).